Angiopoietin-2, an Angiogenic Regulator, Promotes Initial Growth and Survival of Breast Cancer Metastases to the Lung through the Integrin-linked Kinase (ILK)-AKT-B Cell Lymphoma 2 (Bcl-2) Pathway*

Yorihisa Imanishi[‡§¶], **Bo Hu**[‡||1], **Gutian Xiao**[‡**], **Xuebiao Yao**[‡‡§§], and **Shi-Yuan Cheng**[‡§2]

*From the ‡Cancer Institute, §Department of Pathology, ||Department of Medicine, and **Department of Microbiology & Molecular Genetics, University of Pittsburgh School of Medicine, Pittsburgh, Pennsylvania 15213, the ¶Department of Otorhinolaryngology, Head and Neck Surgery, Keio University, School of Medicine, Shinjuku, Tokyo 160-8582, Japan, the ‡‡Anhui Laboratory of Cellular Dynamics and Chemical Biology, Hefei National Laboratory for Physical Sciences at Nanoscale, Hefei 230027, China, and the §§Department of Physiology, Morehouse School of Medicine, Atlanta, Georgia 30310*

The early onsets of breast cancer metastasis involve cell retention, survival, and resistant to apoptosis and subsequent growth at target vascular beds and tissues in distant organs. We previously reported that angiopoietin-2 (Ang2), an angiogenic regulator stimulates MCF-7 breast tumor metastasis from their orthotopic sites to distant organs through the $\alpha_5\beta_1$ integrin/integrin-linked kinase (ILK)/Akt pathway. Here, by using an experimental tumor metastasis model and *in vitro* studies, we further dissect the underlying mechanism by which Ang2 promotes the initial growth and survival of MCF-7 breast cancer metastasis in the lung of animals. We show that Ang2 increases cell survival and suppresses cell apoptosis through ILK-induced phosphorylation of Akt1, Akt2, and up-regulation of Bcl-2 in breast cancer cells. Inhibition of ILK, Akt1, and Akt2, and their effector Bcl-2 diminishes Ang2-stimulated breast cancer cell survival and Ang2-attenuated apoptosis *in vitro*, and initial survival and growth of breast cancer metastasis in the lung of animals. Additionally, siRNA knockdown of endogenous Ang2 in three human metastatic breast cancer cell lines also inhibits phosphorylation of Akt, expression of Bcl-2, and tumor cell survival, migration, and increases cell apoptosis. Since increased expression of Ang2 correlates with elevated potential of human breast cancer metastasis in clinic, our data underscore the importance that up-regulated Ang2 not only stimulates breast cancer growth and metastasis at late stages of the process, but is also critical at the initiating stages of metastases onset, thereby suggesting Ang2 as a promising therapeutic target for treating patients with metastatic breast cancer.

Breast cancers are the most common tumors in humans that inflict women with ~210,000 new cases in 2010 within the United States with poor prognosis. The major cause of breast cancer death is not due to local tumors but distant tumor metastases that are often undiscovered during initial diagnosis and are resistant to conventional therapies (1). Breast cancer metastasis is a multistage process during which tumor cells spread from the primary tumor sites to distant organs. Acquisition of a metastatic phenotype by breast cancer cells alters multiple signal pathways that induce cell motility, invasion into peripheral tissues and entrance into the circulation, promote cell survival in the new microenvironment and subsequent growth of secondary tumors in their target organs (2, 3). Studies of gene discovery have identified the determinants of gene signatures and critical pathways that induce and promote breast cancer metastasis to distant organ sites (4). However, the molecular mechanisms underlying the breast cancer metastatic process, especially during initial onset of tumor metastasis at distant organs remains largely unknown (5).

Angiopoietins (Ang)[3] are Tie2 receptor ligands that play important roles in vascular development, vessel remodeling, and angiogenesis (6). Ang2 was initially identified as an antagonist for Ang1 activation of Tie2 that modulates vessel stability (7). However, accumulating evidence demonstrated a link of increased expression of Ang2 with invasive and metastatic phenotypes of various types of human cancers including breast cancers (8, 9). Ectopic expression of Ang2 by various types of cancer xenografts promoted tumor angiogenesis, growth, invasion, and metastasis in animals (8–10). Moreover, preclinical investigations demonstrated that selective inhibition of tumor-derived Ang2 by specific reagents suppresses tumor angiogenesis and growth by inducing vessel normalization and preventing VEGF-stimulated neovascularization in animals (11, 12). Significantly, combination inhibition of Ang2 and VEGF or VEGFR-2 further reduces tumor angiogenesis and growth, accompanied with decreased tumor cell proliferation and increased apoptosis (13–16). Therefore, targeted inhibition of

[1] To whom correspondence may be addressed. Tel.: 412-623-7791; Fax: 412-623-4840; E-mail: hub@upmc.edu.

[2] To whom correspondence may be addressed: Cancer Institute & Department of Pathology, Research Pavilion at Hillman Cancer Center, Suite 2.26, 5117 Centre Ave., Pittsburgh, PA 15213-1863. Tel.: 412-623-3261; Fax: 412-623-4840; E-mail: chengs@upmc.edu.

[3] The abbreviations used are: Ang, angiopoietin; ILK, integrin-linked kinase.

Angiopoietin-2 Promotes Initial Tumor Metastases

Ang2 and other angiogenic signaling such as the VEGF/VEGFR pathway presents attractive therapeutic options for treating patients with breast cancers (6, 9).

We have previously reported that ectopic expression of Ang2 by human breast cancer MCF-7 cells that show low potential of tumor growth and metastasis, significantly promote cancer metastases of primary breast tumors from orthotopic sites to several distant organs of mice (10). However, our study focused on the impacts of the Ang2-$\alpha_5\beta_1$ integrin-integrin-linked kinase (ILK)/Akt/GSK-3β signaling on the final outcomes of enhanced breast cancer metastasis. Because first steps of breast cancer metastasis are comprised initial tumor cell survival and growth in the distant organs such as in the lung (2, 3), in this report, using an experimental tumor metastasis mouse model and *in vitro* studies, we aimed to gain better understanding of Ang2 stimulation of breast cancer lung metastasis in the initial onsets. We show that ectopic expression of Ang2 by MCF-7 cells increased tumor cell survival and growth in the lung at the first 24 h up to 8 days post-injection of tumor cells through the Ang2/ILK/Akt/Bcl-2-mediated pathway. Inhibition of ILK, Akt1/2, and Bcl-2 by siRNAs significantly abrogated Ang2-stimulated breast cancer cell survival under stress conditions *in vitro* and in the lung of mice, thereby suppressing breast cancer metastasis to the lung of animals.

MATERIALS AND METHODS

Cell Lines and Reagents—Human MCF-7, MDA-MB-231, MDA-MB-468, and SK-BR-3 breast cancer cells were obtained from ATCC, and clone 1834 cells derived from MDA-MB-231 cells were from Dr. J. Massague at Memorial Sloan-Kettering Cancer Center, New York. These cells were cultured as previously described (10, 17, 18). The following antibodies were used for this study: goat anti-Ang2 antibody (AF623, R&D Systems, Minneapolis, MN); mouse anti-phospho-Akt (Ser-473; 587F11), rabbit anti-Akt (11E7), anti-phospho-Akt (Ser-473, 193H12), anti-phospho-Akt (Thr-308; 244F9), anti-phospho-Bad (Ser-136, D25H8), and anti-Bax (D2E11) antibodies (Cell Signaling, Danvers, MA); rabbit anti-ILK, anti-Akt1, and anti-Akt3 antibodies (Upstate Biotechnologies, Lake Placid, NY); mouse anti-Akt2 (F-7), rabbit anti-Bad (C-7), anti-Bcl-2 (N-19), and anti-β-actin (I-19) antibodies (Santa Cruz Biotechnology, Santa Cruz, CA); peroxidase-conjugated anti-rabbit, anti-mouse, and anti-goat antibodies (Dako, Carpinteria, CA). Other chemicals and reagents were from Thermo Fisher Scientific (Hanover Park, IL), Bio-Rad, Sigma Chemicals, or Invitrogen (Carlsbad, CA). MCF-7 cell lines that stably express Ang2 and GFP, expression, and purification of Ang2 and immunoblot (IB) and immunoprecipitation (IP) are described in detail in our previous reports (10, 19).

Xenograft Assays—All animal work was performed in accordance with NIH guidelines under the protocol approved by the Institutional Animal Care and Use Committee at University of Pittsburgh. In an experimental metastasis model, 1×10^6 of MCF-7 control GFP, Ang2#1 or Ang2#52 cells (referred as to Ang2#1 and Ang2#52 hereafter) were separately injected into the tail veins of 8-week-old ovariectomized female nude mice (Taconic, Germantown, NY) supplemented with 17 β-estradiol (E_2) pellets (60-day slow release; Innovation Research of Amer-

ica, Sarasota, FL). Mice were euthanized 12–14 weeks post-injection or when pathological symptoms developed. The lung, liver, spleen, kidney, ovary, bone, lymph nodes, and brain were removed, processed, and sectioned as previously described (10). Metastasis in the organs was first determined by direct epifluorescent examination of GFP-positive cells using an Olympus SZX12 stereomicroscope before embedding in OCT, and an Olympus BX51 microscope after cryo-sectioning, and then followed by H&E staining using their sister sections. Images were then captured with SPOT digital cameras (Diagnostic Instrument) equipped on these microscopes.

In Vivo Cell Survival Assays—To evaluate cell survival, 2×10^6 of control/GFP or Ang2#1/GFP MCF-7 cells were separately injected into the tail veins of nude mice supplemented with 21-day release 17-β-E_2 pellets. The cells transfected with indicated siRNAs were injected into the tail veins of animals 72 h after transfection. At each indicated time point after injection, 4 mice per each group were euthanized and the lungs were harvested. Images of 10 random frames per lung were captured under an epifluorescent stereomicroscope (Olympus SXZ12) at $\times108$ magnification and analyzed by counting the numbers of GFP-positive cells within the area using the Image Pro Plus software (Version 4.1; Media Cybernetics). The percentage of metastatic cell survival was determined by normalizing the mean numbers of cells at each indicated time point with those at 4 h for each group. Difference of the percent cell survival at each time point was statistically analyzed using Mann-Whitney U test.

In Vivo TUNEL Assays—To examine apoptotic tumor cells in the lung of mice described above, 8 μm cryostat sections of the lungs were analyzed using the *in situ* Cell Detection Kit, TMR red (Roche Applied Science, Indianapolis, IN). The assay was performed according to the manufacturer's instructions, followed by counterstaining with Hochest 33258. Images of 10 random frames per section were captured at $\times200$ magnification and analyzed to calculate the apoptotic index (AI) of tumor cell as a ratio of apoptotic tumor cell number to total GFP-positive tumor cell number. Difference of AI of tumor cells at each time point was statistically analyzed using a *t* test.

In Vitro Cell Survival Assays—MCF-7 control GFP, Ang2#1, and Ang2#52 cells were grown in media containing 10% FBS until 80% confluence, followed by in a serum-free/phenol red-free medium for 48 h. Then, the cells were trypsinized, counted, separately seeded at 4×10^5 cells/well in 6-well plates. Control GFP or Ang2#1 cells transfected with indicated siRNAs were prepared similarly 72 h after transfection without preserum-starvation. The cells were incubated with serum-free/phenol red-free media, or with 10% charcoal-treated FBS/phenol red-free media containing 100 μM cobalt chloride ($CoCl_2$, Sigma) to mimic hypoxia condition (20) in the presence or absence of 1.0 or 5.0 μM of HA 14−1 (an inhibitor for Bcl-2) for various time periods as indicated. The numbers of survival cells at each time point were analyzed by trypan blue dye exclusion, counted, and normalized to the number of the cell seeded on day 0.

In Vitro Migration Assays—*In vitro* migration and invasion assays were performed as previously described (10). Briefly, various serum-starved breast cancer cells that were transiently transfected with a siRNA pool for Ang2 or control siRNAs were

separately suspended at 1×10^6 cells/ml in serum-free DMEM containing 0.5% BSA. 50 μl of each cell suspension was seeded into upper wells of the Boyden chambers. The cells were then allowed to migrate through the 12 μm pore size membranes precoated with gelatin for 12 h at 37 °C. After the membrane was fixed and stained, non-migrating and non-invading cells were removed. The number of migrating cells and invading cells was quantified under a microscope (10).

Cell Death Detection ELISA—Cytoplasmic cell extracts were prepared and normalized on the basis of total cell number of both alive and dying cells. Cell apoptosis was measured in triplicate by quantification of cytoplasmic histone-bound DNA fragments using a cell death detection ELISA kit (Roche Applied Science) according to the manufacturer's instructions. The results were shown as relative apoptosis by normalizing each absorbance value to that of each control.

Knockdown of ILK, Ang2, Akt1, Akt2, and Bcl-2—ILK siRNA (5′-AAGGACACAUUCUGGAAGGGG-3′) (21) and siRNA pools for Ang2 and Bcl-2 were from Dharmacon, Lafayette, CO. The 25-nucleotide StealthTM siRNA for Akt1 (5′-ACGUCG-GAGACUGACACCAGGUAUU-3′), Akt2 (5′-GGCACGGGC-UAAAGUGACCAUGAAU-3′) (22) and StealthTM RNAi negative control medium GC duplex were from Invitrogen, San Diego, CA. MCF-7 control GFP and Ang2#1 cells, MDA-MB-231, clone #1834, MDA-MB-468 and SK-BR-3 were separately transfected with siRNAs for control (C), ILK (I), Akt1(A_1), Akt2 (A_2), Akt1+Akt2 ($A_{1\&2}$), Ang2 (A), and Bcl-2 (B) using Lipofectamine 2000 (Invitrogen) according to the manufacturer's protocol. Efficacies of specific knockdown of ILK, Akt1, Akt2, Ang2, and Bcl-2 in the transfected cells were confirmed by IB analyses.

RESULTS

Expression of Exogenous Ang2 Enables MCF-7 Breast Cancer Cells to Metastasize to Several Distant Organs of Animals—In our previous study, we described a significant correlation between up-regulation of Ang2 and metastatic potential, tumor grade, and lymph-vascular invasion during human breast cancer progression. By overexpression of exogenous Ang2 at levels comparable with that detected in clinical human breast cancer specimens in poorly metastatic MCF-7 breast cancer cells, we demonstrated that Ang2 stimulates breast cancer metastasis from orthotopic sites (mammary fat pads) to various organs including the lung through the $\alpha_5\beta_1$ integrin-ILK pathway (10). Because the early steps of tumor metastasis decide the fate of metastatic cancer cells after arrival at distant organs, in this study, we aimed to dissect the mechanisms by which Ang2 promotes initial growth and survival of metastatic MCF-7 cells in the lung of animals using an experimental metastatic xenograft model. We first sought to determine whether Ang2 stimulation of MCF-7 breast cancer metastasis is involved in the initial onset of tumor metastasis. We intravenously administered MCF-7 Ang2/GFP-expressing and control/GFP-expressing cells into the tail veins of nude mice. Twelve to 14 weeks post-injection, the mice were euthanized and various organs of the mice were examined. As summarized in Fig. 1A, expression of Ang2 by MCF-7 cells (Ang2#1 and Ang2#52) stimulated breast cancer metastases to the lung, liver, spleen, and ovary with a preference to the lung of mice. In contrast, injection of GFP-expressing (MCF-7) control cells did not cause any observable metastatic tumor growth in these organs. As illustrated in Fig. 1B, the metastatic tumors were grossly visible on the surfaces of lung (Fig. 1B, *panels e* and *i*). Micrometastatic Ang2#1 and Ang2#52 tumor cells could be found directly as green foci in gross tissues of the lung (Fig. 1B, *panels f* and *j*). Cryosections of the lung tissues under epifluorescence (*panels d, h,* and *l*) and H&E staining of identical sections (panel *c, g,* and *k*) further validated our observation. In contrast, no metastatic tumor foci were detected in the organs including the lung of mice that received MCF-7 control GFP cells (Fig. 1, *A* and *B*). In an agreement with our previous report (10), the frequency of tumor metastasis to various organs in these mice correlates with the expression levels of Ang2 in MCF-7 cells. Ang2#1 cells express Ang2 at high levels and Ang2#52 cells express Ang2 at medium levels while Ang2 was undetectable in MCF-7 control GFP cells (10). Mice received Ang2#1 cells displayed higher incidence (91%) of tumor metastasis than that in mice received Ang2#52 cells (75%).

Ang2 Enhances Initial Growth of Metastatic MCF-7 Tumors in the Lung by Stimulation of Cell Survival and Inhibition of Cell Apoptosis—To determine the effects of expression of Ang2 by MCF-7 cells on initial onset of the experimental tumor metastasis, a total of 24 mice in two groups with 4 mice at each time point that separately received Ang2#1 or GFP cells were euthanized at 4, 12, 24, 48 h, 5 and 8 days post-injections. Various GFP-expressing cells in the lung of each mice at each time point were evaluated (Fig. 2A) and statistically quantified as percentage cells of each group and each time point compared with that at 4 h post-injections (Fig. 2B). As shown in Fig. 2A, within the first 4 h, Ang2#1 and control GFP (MCF-7) cells were efficiently retained in the lungs of mice (Fig. 2A; 4 h). However, the number of the cells in the lung of mice in both groups was rapidly decreased at 12 h post-injections. Although the cell numbers in each group were further declined at 24 h post-injections, marked differences in number of tumor cells retained in the lung of mice between two groups were observed at 24 and 48 h of post-injections. Compared with that at 4 h in both groups, at 24 h post-injection, $28.3 \pm 3.3\%$ of Ang2#1 cells *versus* $11.0 \pm 3.7\%$ of GFP cells and at 48 h, $3.2 \pm 1.2\%$ of Ang2#1 cells *versus* $0.9 \pm 0.5\%$ of GFP cells were retained in the lung, respectively. Significantly, at 5 and 8 days post-injection, the retained/survived Ang2#1 cells started to grow forming green foci or colonies, indicating an initial growth of tumor micro-metastasis in the lung. In contrast, minimal numbers of MCF-7 control GFP cells were found as single cells in the lung in both time points (Fig. 2, *A* and *B*) and eventually failed to survive and grow to metastatic tumors (Fig. 1). In this experimental tumor metastasis model, between 12 and 48 h post-injection, we could not determine whether the rapidly decreased GFP-expressing cells in both groups was due to the flush by the circulating blood or tumor cells were not able to survive. To assess the cell survival of breast tumor cells retained in the lung, we performed *in vivo* TUNEL assay at 12 and 24 h post-injections. As shown in Fig. 2, *C* and *D*, although no difference in apoptotic index of control GFP (MCF-7, $10.8 \pm 3.6\%$) *versus* Ang2#1 (8.4 ± 1.8) cells was found in the lungs at 12 h post-injection, a significantly higher

A.

Incidence of Organ Metastases

Cell lines	No. of mice	No. of mice with any metastases		No. of mice with metastases			
				Lung	Liver	Spleen	Ovary
MCF-7	7	0	(0%)	0	0	0	0
Ang2#1	22	20	(91%)*	19	5	2	1
Ang2#52	8	6	(75%)*	6	0	0	0

B.
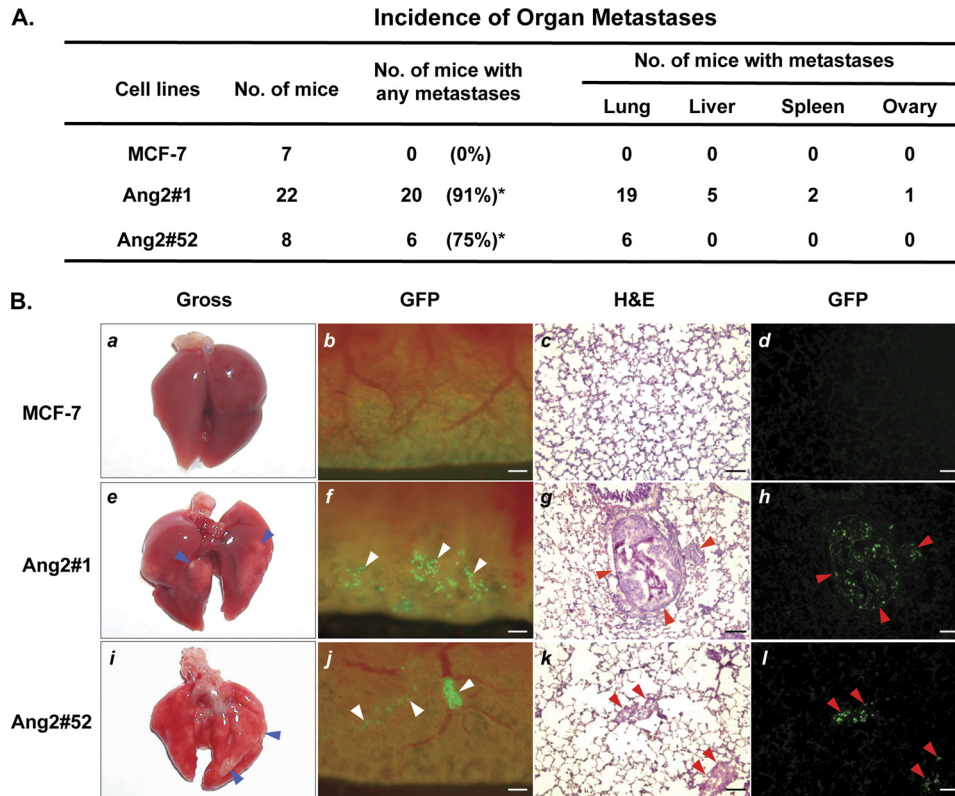
FIGURE 1. **Expression of exogenous Ang2 enables MCF-7 breast cancer cells to metastasize to several organs of mice.** *A*, summary of the incidence of organ metastases in mice that separately received MCF-7 Ang2-expressing (Ang2#1 or Ang2#52) or GFP-expressing (MCF-7) cells. Fisher's exact test showed significantly higher incidence of metastasis in mice received Ang2#1 cells (*, $p < 0.0001$) or Ang2#52 (*, $p = 0.007$) as compared with mice received MCF-7/GFP cells. Data are combined from two independent experiments with 3–11 mice per group. *B*, representative images of the lungs of mice in *A* analyzed by different methods. MCF-7 breast cancer metastases in the lung of mice were examined 12–14 weeks after tail-vein injection by gross observation (*panels a, e, and i*) and epi-fluorescent observation of GFP (*panels b, f, and j*). Cryo-sections were further examined by epi-fluorescence (*panels d, h, and l*) followed by H&E staining (*panels c, g, and k*). Mice that received Ang2 #1 or Ang2#52 cells showed lung metastases (*panels e to l*) with a high incidence. Grossly visible metastases (*blue arrowheads*) in the lung (*panels e and i*) were identified as green foci (*panels f and j, white arrowheads*) and cells expressing GFP in the nuclei (*panels h and l, red arrowheads*), and further confirmed by H&E staining (*panels g and k, red arrowheads*). Scale bars: *panels b to d, f to h,* and *j to l,* 120 μm. Data are representative from two independent experiments shown in *A* with similar results.

number of apoptotic cells of control GFP cells (35.4 ± 5.2%) than that of Ang2#1 cells (11.7 ± 3.0%) was observed 24 h after the cells entered circulation, suggesting that increased cell death contributed to the rapid loss of MCF-7 cells in the lungs of mice and overexpression of Ang2 protects MCF-7 cells from apoptosis in the lung. Taken together, these results show that expression of Ang2 by MCF-7 cells augments cell survival, suppresses cell apoptosis in the lung of mice on the initiating stage of onset of metastases, which contributes to initiation of tumor growth of breast cancer micrometastases in multiple distant organs (Fig. 1*A*).

Ang2 Augments Cell Survival and Suppresses Apoptosis of MCF-7 Cells under the Stress Conditions—Next, we tested whether Ang2 promotes breast cancer cell survival under the conditions of growth stress. As shown in Fig. 3*A*, under serum-starvation conditions, compared with cells at day 0 post-treatment, at days 4 and 6, Ang2#1 cells displayed a survival rate of 76.7 ± 5.7% and 49.8 ± 4.5%, Ang2#52 cells showed 67.2 ± 4.5% and 46.5 ± 6.3% whereas control GFP (MCF-7) cells only had a survival rate of 47.5 ± 6.9% and 26.5 ± 3.1%, respectively. Similarly, at day 4, compared with control GFP cells, Ang2#1 cells showed apoptotic index of 69.9 ± 3.3% and Ang2#52 cells had 78.9 ± 1.9%, respectively (Fig. 3*B*). As shown in Fig. 3*C*, when various cells exposed to cobalt chloride (CoCl$_2$), a

hypoxia-mimetic agent (20) in cell culture, 100 μM of CoCl$_2$ (23) caused a rapidly decrease in survival of control GFP cells (MCF-7, from 45.9 ± 3.1% at day 2 to 9.4 ± 1.8% at day 8) whereas Ang2 expression significantly promoted cell survival (94.1 ± 3.1% for Ang2#1 cells and 90.9 ± 1.3% for Ang2#52 cells at day 2; 38.1 ± 2.7% for Ang2#1 and 32.8 ± 1.3% for Ang2#52 cells at day 8, respectively). Furthermore, Ang2 also suppressed CoCl$_2$-induced cell apoptosis at day 4. Ang2#1 cells had 35.7 ± 1.7% and Ang2#52 cells had 55.0 ± 2.2% apoptotic index compared with that of MCF-7 control cells (Fig. 3*D*). However, we did not observe significant differences of growth rate of these two groups of MCF-7 Ang2-expressing cells under complete media containing 10% FBS. Nonetheless, these results suggest that Ang2 augments cell survival and attenuates cell apoptosis of breast cancer cells under the stress conditions *in vitro*.

Ang2 Activates Akt1 and Akt2 and Induces Expression of Bcl-2 in MCF-7 Cells—Because Akt is phosphorylated by ILK, the mTORC2 complex and DNA-dependent protein kinase (DNA-PK) at Ser-473 (p-Akt^{Ser473}) and by PDK1 at Thr-308 (p-Akt^{Thr308}) (24, 25) and Ang2 induces p-Akt^{Ser473} through the $\alpha_5\beta_1$ integrin-ILK signaling (10), we examined whether Ang2 activates Akt to promote tumor cell survival and inhibit cell apoptosis under serum-starvation condition. As shown in Fig. 4*A*, in absence of serum, expression of Ang2 by MCF-7 cells
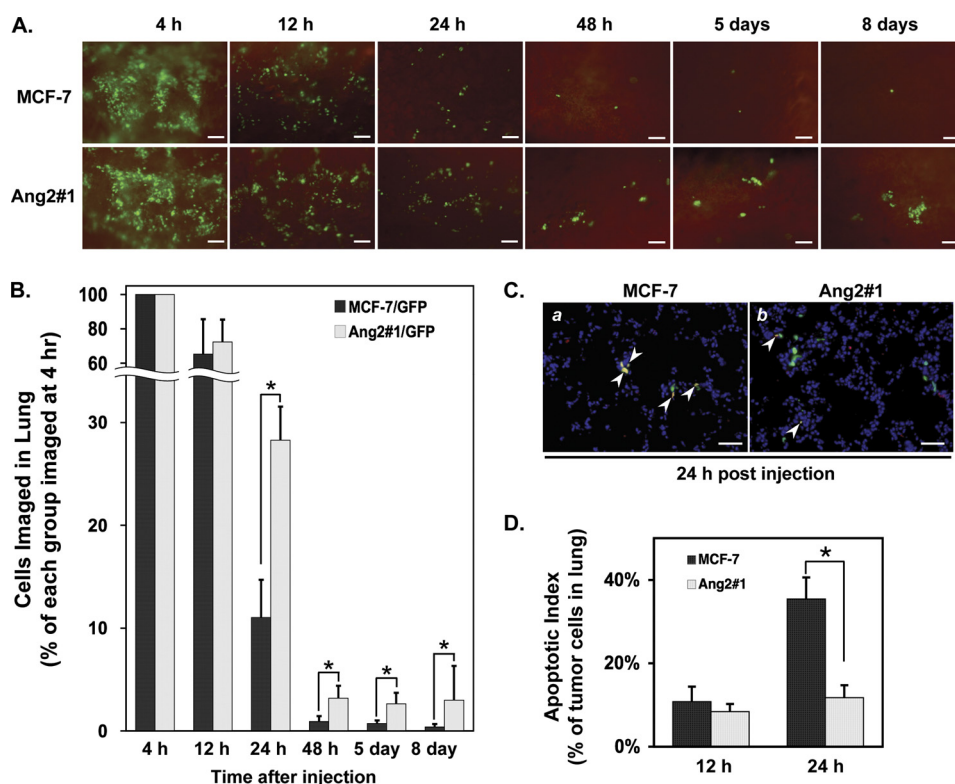
FIGURE 2. **Ang2 enhances breast cancer cell survival, suppresses apoptosis, and promotes the initial growth of breast cancer micrometastases in the lung.** *A*, at each indicated time point post-injection, 4 mice per each group were euthanized and the lungs were harvested and examined. Images of 10 random frames per lung were captured under an epifluorescent stereomicroscope (Olympus SXZ12). Representative images of the lung at each time point are shown. Scale bars: 100 μm. *B*, numbers of GFP-expressing cells of each group within the area of 10 random frames per lung were analyzed using the Image Pro Plus software. The percent metastatic cell survival was determined by normalizing the mean numbers of the cells at 12 h or later with those at 4 h for each group. Difference of the percent cell survival at each time point was statistically analyzed using Mann-Whitney U test: *, $p < 0.05$ and error bars: $\pm$ S.D. *C*, representative images of TUNEL assays of MCF-7 tumor cells in the lung 24 h after tail-vein injection. *Green* color, viable GFP-expressing tumor cell nuclei; *red* color, total apoptotic cell nuclei, and *blue* color, cell nuclei. *Yellow* color, merged of green- and red-stained apoptotic tumor cell nuclei (*arrowhead*); Scale bars: 50 μm. *D*, apoptotic index of tumor cells in the lungs 12 and 24 h after tail-vein injection was statistically analyzed using *t* test: *, $p < 0.001$ and error bars: mean $\pm$ S.D. Data in *A–D* are representative of three independent experiments with similar results.

stimulated p-Akt^{Ser473} (Ser-473) but not p-Akt^{Thr308} (Thr-308) at both 24 and 48 h post-treatment compared with that of MCF-7 control cells. When MCF-7 control cells were exposed to polylysine (poly-L, a non-stimulative substrate for integrins), recombinant Ang2 proteins or fibronectin (FN) pre-coated in cell culture plates, Ang2, but not poly-L or FN induced p-Akt^{Ser473} but not p-Akt^{Thr308} (Fig. 4*B*). Ang2 induction of p-Akt^{Ser473}, but not p-Akt^{Thr308} validates our previous observation that Ang2 induces p-Akt^{Ser473} through the $\alpha_5\beta_1$ integrin-ILK signaling (10).

Because Akt isoforms displayed distinct roles in promoting the initiation and metastatic phases of breast tumor progression (26), we determined Ang2 stimulation of Akt isoforms in MCF-7 cells. As shown in Fig. 4*C*, while expression of Ang2-induced p-Akt^{Ser473} in MCF-7 cells, expressions of Akt1 and Akt2 but not Akt3 were detected in MCF-7 cells and exogenous expression of Ang2 did not change the expression levels of Akt1 and Akt2 in MCF-7 cells. Furthermore, expression of Ang2 induced p-Akt^{Ser473} of Akt1 and Akt2 but not Akt3 in MCF-7 cells (Fig. 4*D*). Additionally, we examined the impact of Ang2 on three death molecules downstream of Akt, Bcl-2, Bcl-2-associated agonist of cell death (Bad), and Bcl-2-associated X protein (Bax) (25). We found that Ang2 markedly induced expression of Bcl-2 but had no effects on protein expression

or phosphorylation of Bad and protein expression of Bax in MCF-7 cells (Fig. 4*E*).

Ang2 Promotes Cell Survival through ILK-Akt1/2 Signaling—Next, we examined effects of knockdown of ILK on p-Akt^{Ser473}, expression of Bcl-2 and cell survival and apoptosis of Ang2-expressing and control MCF-7 cells. As shown in Fig. 5*A*, depletion of ILK expression by a siRNA pool markedly suppressed Ang2-induced p-Akt^{Ser473} but not p-Akt^{Thr308}, and expression of Bcl-2, indicating that Ang2 induces p-Akt^{Ser473} and Bcl-2 through ILK. As expected, knockdown of ILK decreased Ang2-stimulated cell survival (Fig. 5*B*, cell survival, compare ILK.siRNA (I) of $102.5 \pm 6.6\%$ with control.siRNA (C) of 143.6 ± 3.3 for Ang2#1, I of $103.1 \pm 5.7\%$ with C of $132.1 \pm 7.8\%$ for Ang2#52) and increased cell apoptosis (Fig. 5*C*, cell apoptosis, compare I of $93.5 \pm 6.9\%$ with C of 62.1 ± 8.4 for Ang2#1 and I of $95.6 \pm 7.6\%$ with C of $72.3 \pm 6.7\%$ for Ang2#52).

To determine whether Akt1 or Akt2 or both mediates Ang2 stimulation, we use specific siRNAs to knock down of Akt1 and Akt2, individually or together in Ang2#1 cells. As shown in Fig. 5*B*, separate inhibition of Akt1 (A_1) or Akt2 (A_2) attenuated Ang2-induced protein expression of Bcl-2 whereas simultaneous depletion of both Akt1 and Akt2 ($A_{1\&2}$) by siRNAs showed profound suppression of Ang2-induced expression of Bcl-2 (Fig. 5*D*). To similar extents, separate knockdown of Akt1 (A_1)
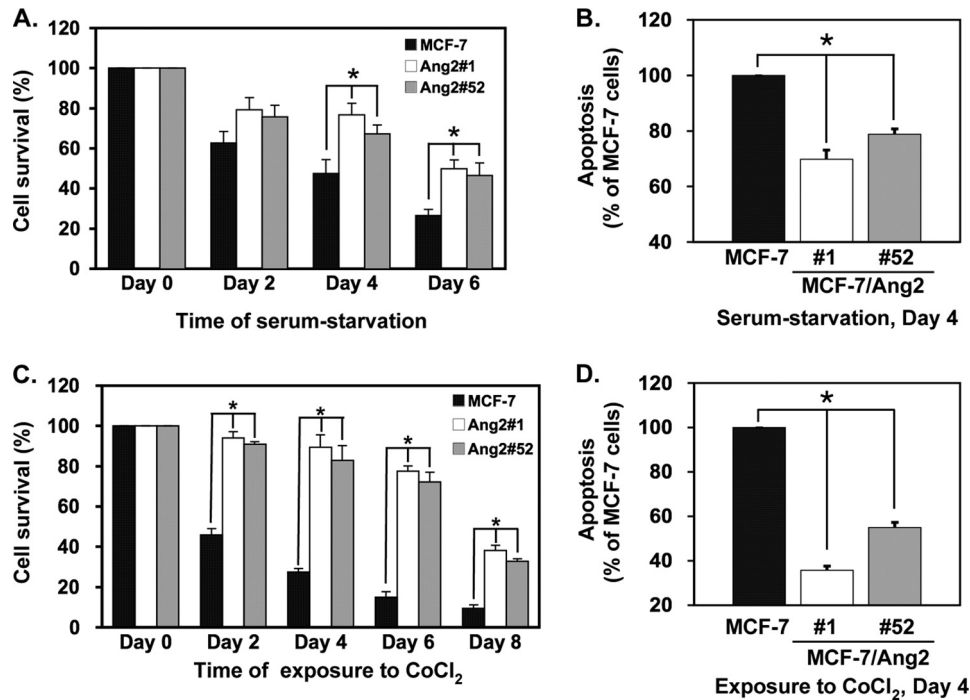
FIGURE 3. **Ang2 augments cell survival and suppresses cell apoptosis of MCF-7 cells *in vitro* under the conditions of growth stress.** MCF-7 control GFP cells, Ang2#1 and Ang2#52 cells were incubated with serum-free/phenol red-free medium as serum-starvation model (*A*) and (*B*) or with 10% charcoal-treated FBS/phenol red-free medium containing 100 μM of cobalt chloride ($CoCl_2$) as a hypoxia model (*C* and *D*). In *A* and *C*, the numbers of survival cells at each time point were analyzed by trypan blue dye exclusion, counted, and normalized to the cell number of each group seeded on day 0. In *B* and *D*, apoptosis in the cells cultured under serum-starvation (*B*) or a hypoxia condition (*D*) for 4 days were analyzed using a cell death detection ELISA kit. Data were shown as relative apoptosis by normalizing each absorbance value to that of MCF-7 control cells. All data were statistically analyzed using *t* test. *, $p < 0.001$ and error bars: mean $\pm$ S.D. Results in *A*–*D* are representative of three independent experiments with similar results.

or Akt2 (A_2) decreased Ang2-stimulated cell survival or induced cell apoptosis at moderate levels whereas double depletion of Akt1 & Akt2 ($A_{1\&2}$) further inhibited cell survival or enhanced cell apoptosis (Fig. 5*E*, cell survival, compare $A_{1\&2}$ of $34.6\% \pm 6.1$ with A_1 of $66.4 \pm 7.4\%$ or A_2 of $81.3 \pm 5.1\%$; Fig. 5*F*, cell apoptosis, compare $A_{1\&2}$ of $199.8 \pm 6.6\%$ with A_1 of $154.8 \pm 8.9\%$ or A_2 of $123.4 \pm 7.4\%$). Taken together, these results suggest that both Akt1 and Akt2 contribute to Ang2 modulation of breast cancer cell survival and apoptosis and simultaneous inhibition of Akt1 and Akt2 by siRNA knockdown display marked inhibition of Ang2 stimulation of breast cancer cells.

Knockdown of Akt1 and Akt2 Diminishes Ang2-stimulated Cell Survival and Proliferation of MCF-7 Cells in Vitro and in the Lung of Animals—Afterward, we determined the effects of knockdown of Akt1+Akt2 (siRNA $Akt_{1\&2}$) on Ang2-enhanced cell survival of MCF-7 cells *in vitro* and in the lung of mice. As shown in Fig. 6*A*, compared with control siRNA, knockdown of Akt1 + Akt2 with their corresponding siRNA pools ($Akt_{1\&2}$) effectively inhibited Ang2-induced p-Akt^{Ser473} and expression of Bcl-2 in Ang2#1 cells. As shown in Fig. 6, *B* and *C*, when these siRNA transfected cells were used to assess the impact on cell survival, after 6 day cell culture in absence of serum, compared with cells at day 0 in culture, Ang2#1 cells displayed an increase in cell survival rate of $43.5 \pm 3.6\%$ whereas MCF-7 control cells only had a survival rate of $20.8 \pm 1.8\%$ of cells. To a similar extent, when various cells were treated with $CoCl_2$, Ang2#1 cells displayed a survival rate of $63.6 \pm 3.0\%$ whereas MCF-7 control cells had a survival rate of $22.3 \pm 2.1\%$. However, when

Akt1 and Akt2 were simultaneously knocked down, Ang2-promoted cell survival was diminished under both stress conditions (Fig. 6, *B* and *C*, right halves of the bar graphs). Furthermore, as shown in Fig. 6, *D* and *E*, at 24 h post-injection, mice that received Ang2#1 cells transfected with control siRNAs had $33.5 \pm 11.1\%$ cells retained in the lung compared with that at 4 h whereas mice injected with Ang2#1 cells in which endogenous Akt1 and Akt2 were knocked down by siRNAs only had $3.8 \pm 0.8\%$ of cells left in the lung. After 5 days, mice received Ang2#1 cells that were transfected with control siRNAs showed $4.3 \pm 1.4\%$ cells stayed in the lung as small tumor cell clusters whereas mice received Ang2#1 cells in which Akt1 and Akt2 were knocked down only had $0.3 \pm 0.3\%$ cell left in the lung (Fig. 6*E*). Taken together, these data further support our observation that Ang2 stimulation of breast cancer cell survival and metastatic MCF-7 tumor growth in the lung (Fig. 1) is mediated by the integrin/ILK/Akt signal pathway.

Inhibition of Bcl-2 Suppresses Ang2-stimulated Cell Survival and Proliferation of MCF-7 Cells in Vitro and in the Lung of Animals—Next, we determined whether Bcl-2, a downstream effector of Akt signaling mediates the Ang2-stimulated MCF-7 breast cancer cell survival and initial growth of tumor metastasis in the lung. Various MCF-7 cells were exposed to 0, 1.0, and 5.0 μM of HA14−1, a pharmacological inhibitor for Bcl-2 that did not significantly affect MCF-7 cell viability (27) under serum starvation condition for 48 h. As shown in Fig. 7, *A* and *B*, compared with MCF-7 control cells, expression of Ang2 enhanced Ang2#1 cell survival (a $40 \pm 4.3\%$ increase) and inhibited cell apoptosis (a $30.7 \pm 3.2\%$ decrease) under serum star-
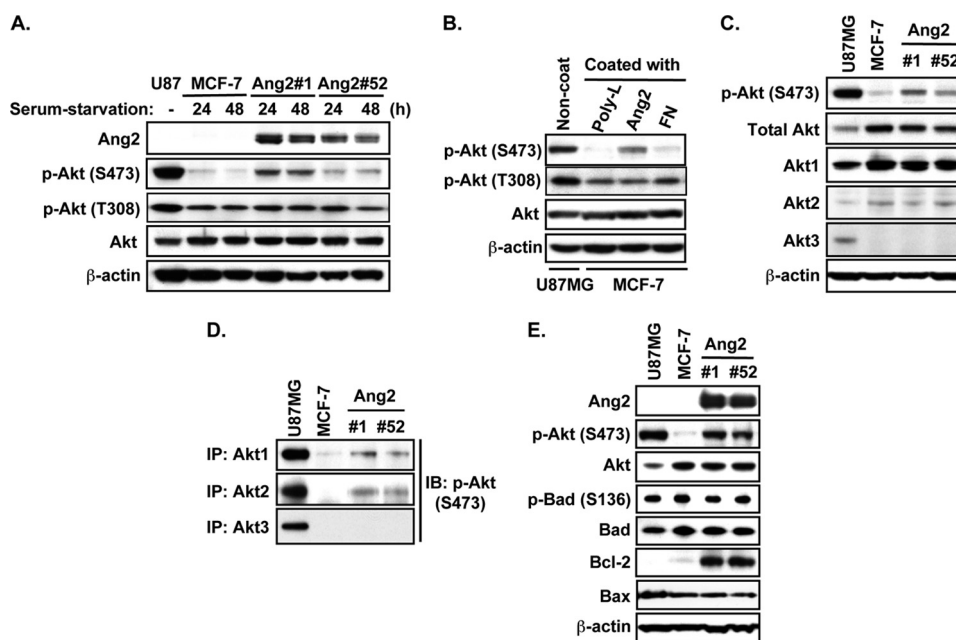
FIGURE 4. **Ang2 stimulates phosphorylation of Akt1 and Akt2 at Ser-473 and induces expression of Bcl-2 in MCF-7 cells.** IB (*A* to *C*, *E*) or IP/IB (*D*) analyses using whole cell lysates of MCF-7 Ang2-expressing cells and control GFP cells with the indicated antibodies. *A*, phosphorylation of Akt at Ser-473 (S473) but not Thr-308 (T308) was enhanced in Ang2-expressing cells compared with MCF-7 control GFP cells under the serum-starvation conditions. *B*, phosphorylation of Akt at Ser-473 (S473) but not Thr-308 (T308) in MCF-7 cells was induced by seeding MCF-7 cells onto recombinant Ang2-coated cell culture plates, but not onto the poly-lysine (poly-L)- or fibronectin (FN)-coated plates. *C*, IB analyses. Expression of Akt1 and Akt2, but not Akt3 was detected in MCF-7 Ang2-expressing and control cells. Expression of exogenous Ang2 induces phosphorylation of Akt at Ser-473 (S473) in MCF-7 cells. *D*, IB/IP analyses. Expression of exogenous Ang2 induces phosphorylation at Ser-473 (S473) of Akt1 and Akt2, but not Akt3 in MCF-7 cells. *E*, IB analyses. Expression of Ang2 enhanced expression of Bcl-2, but not Bax or phosphorylation of Bad in MCF-7 Ang2-expressing cells compared with GFP control cells. In *A* and *C* to *E*, whole cell lysates of phosphatase and tensin homolog (PTEN)-mutated human glioma U87MG cells were used as positive controls for the expression and activation (phosphorylation at Ser-473) of Akt, Akt1, Akt2, and Akt3. Total proteins of Akt and β-actin were used as loading controls for all experiments except *D*. The experiments of *A*–*E* were performed three independent times with similar results.
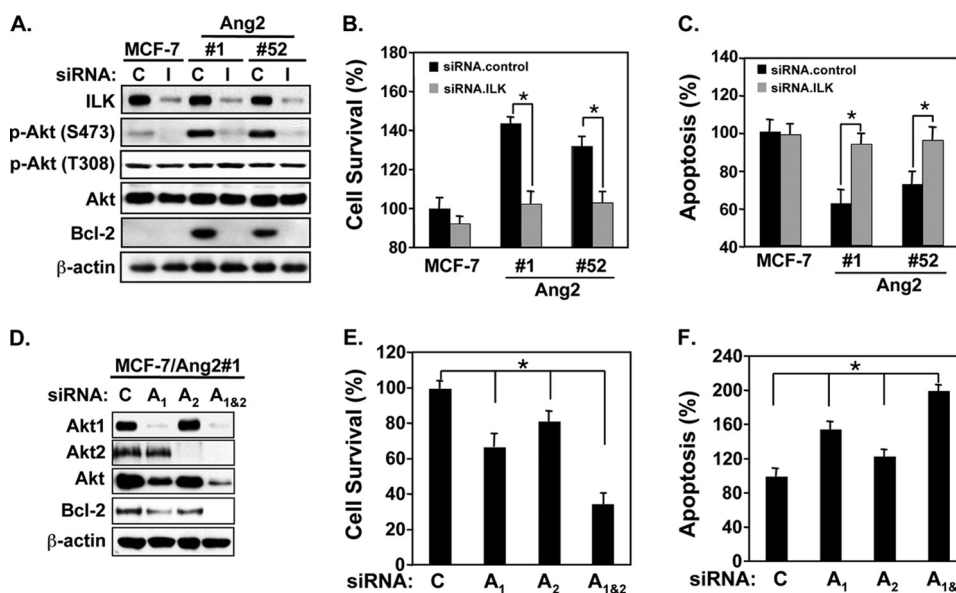

FIGURE 5. **Ang2 enhances cell survival and inhibits cell apoptosis of MCF-7 cells through the ILK-Akt1/2 signaling.** *A* and *D*, IB analyses: knockdown of ILK (I) (*A*) and Akt1 (A$_1$) and Akt2 (A$_2$) separately or together (Akt1 + Akt2, A$_{1\&2}$) by siRNAs (*D*) blocked the Ang2-stimulated phosphorylation of Akt at Ser-473 (S473) but not at Thr-308 (T308) and inhibited the Ang2-induced expression of Bcl-2 in MCF-7 cells. Total proteins of Akt and β-actin were used as loading controls. *B* and *E*, cell survival and *C* and *F*, cell apoptosis in the cells culture under serum-starvation. Ang2#1 cells were separately transfected siRNA pools for control (*C*), siRNA pools for ILK (*I*), Akt1 (A$_1$), Akt2 (A$_2$), or Akt1 + Akt2 (A$_{1\&2}$). 48-h later, the cells were incubated with serum-free/phenol red-free medium (serum starvation) for 4 days. The numbers of survival cells were analyzed by trypan blue dye exclusion, counted and normalized to the cell number of each group seeded on day 0 (*B* and *E*). Cell apoptosis was analyzed using a cell death detection ELISA kit (*C* and *F*). Data of *B*, *C*, *E*, and *F* were statistically analyzed using *t* test. *, *p* < 0.001 and error bars: mean ± S.D. The results of *A*–*F* are representative from three independent experiments with similar results.

vation condition for 2 days (also see Fig. 3, *A* and *B*). While Bcl-2 inhibitor HA14−1 had no impact on cell survival or apoptosis of MCF-7 control cells, HA14−1 at both 1.0 and 5 μM concen-

trations significantly abrogated Ang2-enhanced cell survivals (35.7 ± 3.9% and 39.7 ± 5.1% decreases compared with solvent-treated Ang2#1 control cells, Fig. 7*A*) and diminished the
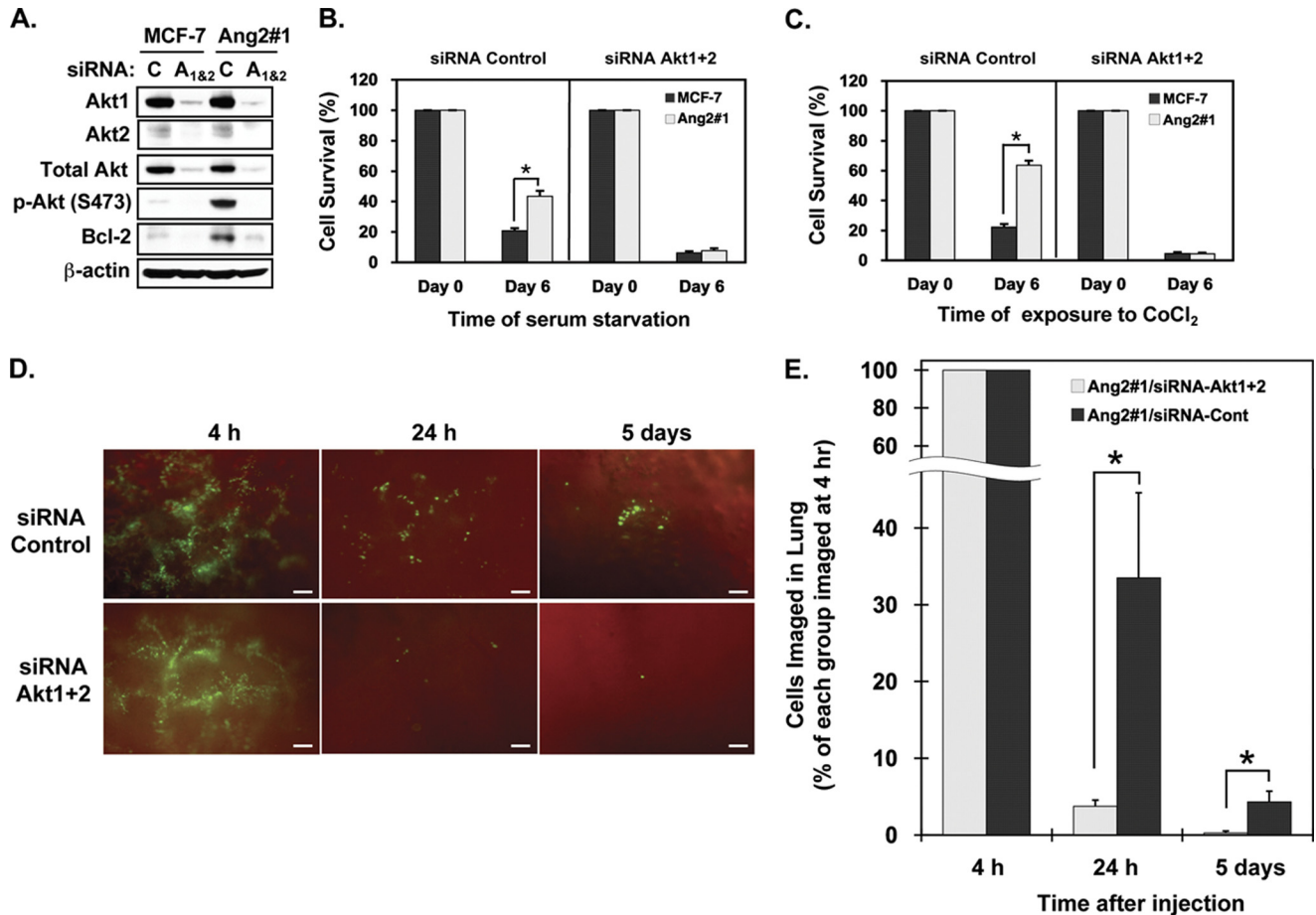
FIGURE 6. **Knockdown of Akt1 and Akt2 diminishes Ang2-stimulated cell survival of MCF-7 cells *in vitro* and in the lung of mice.** *A*, IB analyses: knockdown of Akt1+Akt2 ($A_{1\&2}$) blocked the Ang2-stimulated phosphorylation of Akt at Ser-473 (S473) and Ang2-induced expression of Bcl-2 proteins in Ang2#1 cells. *C*, control siRNAs. Total proteins of Akt and β-actin were used as loading controls. *B* and *C in vitro* cell survival assays. Knockdown of Akt1&Akt2 by siRNAs (siRNA.Akt1 + 2) abrogated the Ang2-enhanced cell survival *in vitro* under serum-starvation condition (*B*) or after the cells were exposed to $CoCl_2$ (*C*). *, $p < 0.001$ by *t* test. Error bars: mean ± S.D. *D*, knockdown of Akt1 + Akt2 (siRNA.Akt1 + 2) in MCF-7 Ang2#1 cells attenuated the Ang2-enhanced cell survival in the lung of mice (4 mice per group) in 24 h and 5 days after the tail-vein injections. Representative images of the lung of various mice at each time point are shown. Scale bars: 100 μm. *E*, percentage of survived breast cancer cells in the lung of mice of each group in *D* was analyzed by normalizing the mean numbers of the cells in 24 h or 5 days after injections with those of each group at 4 h post-injections. Difference of the percentage of cell survival at each time point was statistically analyzed using Mann-Whitney U test. Data in *B*, *C*, and *E*, *, $p < 0.05$ and error bars: mean ± S.D. The results of *A–G* are representative from two or three independent experiments with similar results.

Ang2-attenuated apoptosis (25.3 ± 4.3% and 32.5 ± 3.3% increases compared with solvent-treated Ang2#1 control cells, Fig. 7*B*). To further examine the role of Bcl-2 in Ang2-Akt-stimulated breast cancer cell survival and metastasis, we knocked down Bcl-2 using a siRNA pool in MCF-7/Ang2#1 and control GFP cells (Fig. 7*C*). As expected, depletion of Ang2-up-regulated Bcl-2 markedly attenuated Ang2-promoted cell survival (102.3 ± 6.6% in Bcl-2 siRNA-transfected cells *versus* 135.0 ± 3.3% in control siRNA cells, Fig. 7*D*) and reversed Ang2-suppressed cell apoptosis (94.9 ± 5.4% in Bcl-2 siRNA transfected cells *versus* 64.5 ± 8.7% in control siRNA cells, Fig. 7*E*). In contrast, because minimal levels of Bcl-2 proteins were detected in MCF-7 GFP cells, knockdown of Bcl-2 had minimal impacts on cell survival and apoptosis of control GFP cells (Fig. 7*D*, *left bars*). When these siRNA knockdown cells were injected into the tail veins of mice, as shown in Fig. 7, *F* and *G*, at 24 h post-injection, mice received Ang2#1 cells transfected with control siRNA had 34.7 ± 9.0% cells in the lung compared with that at 4 h post-inoculation whereas mice injected with Bcl-2 knockdown Ang2#1 cells only had 4.3 ± 3.5% cells

retained in the lung. Five days after the injection, mice received Ang2#1/control siRNA had 3.5 ± 0.8% cells remained in the lung as small tumor clusters. In contrast, Ang2#1/Bcl-2 siRNA cells only had 0.1 ± 0.2% cells left in the lung. Taken together, these data demonstrate that the up-regulated Bcl-2 mediates Ang2-promoted MCF-7 breast cancer metastasis through enhancing cell survival and attenuating cell apoptosis in the lung.

Depletion of Endogenous Ang2 by siRNAs in Breast Cancer Cells Inhibits p-Akt[Ser473], Protein Expression of Bcl-2, Cell Survival, Cell Migration, and Increases Cell Apoptosis—Increased expression of Ang2 has been demonstrated to correlate with invasive and metastatic phenotypes of various types of human cancers including breast cancers (8, 9). A previous study showed that endogenous Ang2 proteins are detected at high levels in human breast cancer MDA-MB-468 and SK-BR-3 cells whereas MCF-7 and MDA-MB-231 cells express Ang2 at low levels (17). Therefore, we reasoned that inhibition of endogenous Ang2 in MDA-MB-468 and SK-BR-3 cells would suppress the Akt-Bcl-2 signaling, cell survival, and migration, and
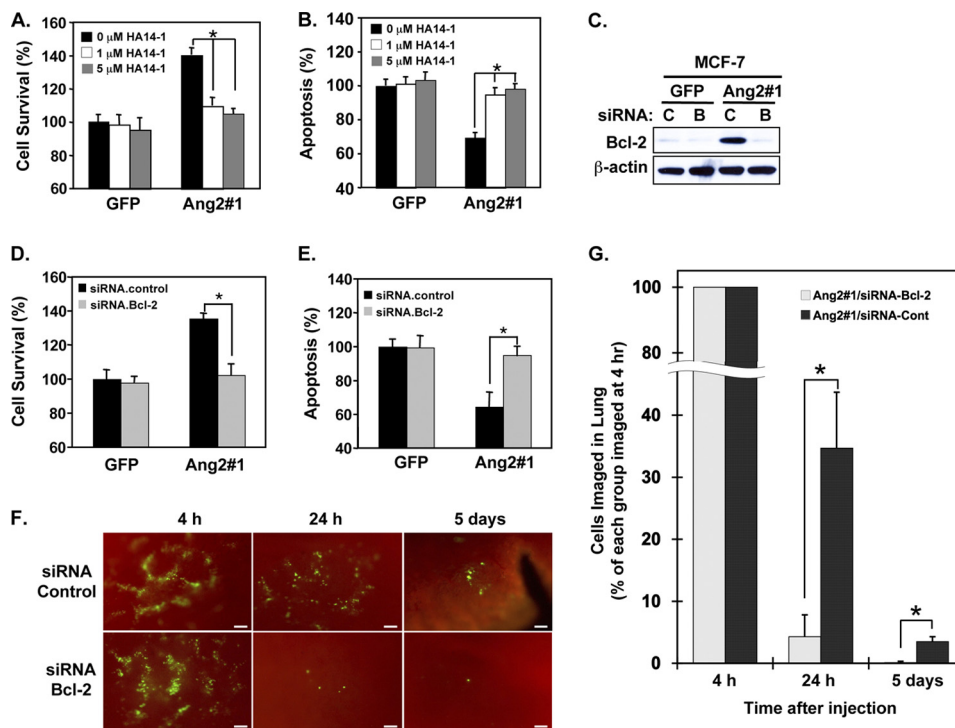
FIGURE 7. **Bcl-2 is a downstream effector of the Ang2-ILK-Akt1/2 signaling that mediates Ang2-enhanced cell survival and Ang2-attenuated cell apoptosis of MCF-7 cells.** *A* and *B*, a pharmacological inhibitor of Bcl-2, HA14–1, significantly inhibited Ang2-enhanced cell survival (*A*) and Ang2-protected cell apoptosis (*B*) under serum-starvation conditions. *, $p < 0.001$ by *t* test and error bars: mean $\pm$ S.D. *C*, IB analyses: knockdown of Bcl-2 with a control (*C*) or siRNA pool for Bcl-2 (*B*) in control GFP or Ang2#1 cells abrogated the Ang2-enhanced cell survival (*D*) and reversed Ang2-attenuated cell apoptosis (*E*) *in vitro* under serum starvation condition (*A*). *, $p < 0.001$ by *t* test. Error bars: mean $\pm$ S.D. *F*, knockdown of Bcl-2 with a siRNA pool (siRNA.Bcl-2) but not the control in Ang2#1 cells attenuated the Ang2-enhanced cell survival in the lung of mice (4 mice per group) in 24 h and 5 days after the tail-vein injections. Representative images of the lung of various mice at each time point are shown. Scale bars: 100 μm. *G*, percentage of survived breast cancer cells in the lung of mice of each group in *F* was analyzed by normalizing the mean numbers of the cells in 24 h or 5 days after injections with those of each group at 4 h post-injections. Difference of the percentage of cell survival at each time point was statistically analyzed using Mann-Whitney U test. *, $p < 0.05$ and error bars: mean $\pm$ S.D. The experiments of *A*–*G* are representative from two or three independent experiments with similar results.

increase cell apoptosis. To this end, we knocked down endogenous Ang2 in these two breast cancer cell lines using a siRNA pool and control siRNAs. As shown in Fig. 8A, depletion of Ang2 inhibited p-Akt[Ser473] and expression of Bcl-2 protein in MDA-MB-468 and SK-BR-3 cells. As expected, when compared with controls, inhibition of endogenous Ang2 in these two cell lines attenuated cell survival (Fig. 8B), cell migration (Fig. 8C), and increased cell apoptosis (Fig. 8D) under serum-starved conditions.

Finally, we validated our observations in a breast cancer MDA-MB-231/#1834 cell clone, an *in vivo*-derived cell population that preferentially metastasize to the lung and several other organs when injected into the tail veins of mice (18). Significantly, gene profile analysis showed that expression levels of Ang2 mRNA is elevated ~20-fold when compared with their parental MDA-MB-231 cells (28). Consistent with the reported data of cDNA arrays, we detected increased levels of endogenous Ang2 proteins in the MDA-MB-231/#1834 cells when compared with that in parental MDA-MB-231 cells (Fig. 9A). We transiently transfected parental and MDA-MB-231/#1834 cells with siRNAs for Ang2 or control. As shown in Fig. 9A, when compared with control siRNAs, depletion of endogenous Ang2 inhibited increased p-Akt[Ser473] and Bcl-2 expression compared with that in parental cells (Fig. 9A), attenuated cell survival (Fig. 9B) and cell migration (Fig. 9C) but increased cell apoptosis (Fig. 9D) *in vitro*, consistent with the data that we

obtained in breast cancer MDA-MB-468 and SK-BR-3 cells (Fig. 8). In contrast, knockdown of Ang2 in parental MDA-MB-231 cells had minimal impact on these cellular behaviors (Fig. 9, *B–D*), possibly because of low levels of endogenous Ang2 in these cells (Fig. 9A). Together, inhibition of endogenous Ang2 in metastatic breast cancer cells impaired the activated Akt-Bcl-2 signaling, cell survival, and migration, and increase cell apoptosis.

DISCUSSION

In this study, we provide novel molecular insights into Ang2 stimulation of breast cancer metastasis to the lung of animals by focusing on initial onset of breast tumor metastasis. We show that at early stages of MCF-7 breast cancer metastasis in the lung, Ang2 stimulates breast cancer metastasis through the ILK-Akt1/2-Bcl-2 signaling, increasing tumor cell survival and suppressing cell apoptosis, resulting in subsequent tumor growth in the lung of animals. Inhibition of ILK, Akt1/2, and Bcl-2 by siRNAs or Bcl-2 by a pharmacological inhibitor abrogates Ang2 stimulation of tumor cell survival *in vitro* under growth stress conditions and Ang2-promoted tumor metastasis in the lung of mice. Conversely, depletion of endogenous Ang2 by siRNAs in three metastatic breast cancer cell lines inhibited the Akt-Bcl-2 signaling, cell survival, and migration, and increased cell apoptosis. Our work demonstrates that increased expression of Ang2 enhances breast cancer cell
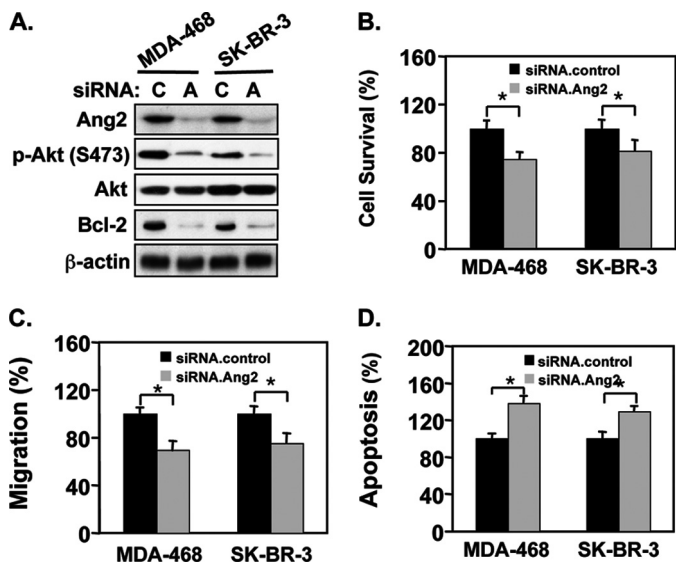
FIGURE 8. **Knockdown of endogenous Ang2 inhibits the Akt-Bcl-2 signaling and decreases cell survival, migration, and inhibits cell apoptosis of MDA-MB-468 and SK-BR-3 cells *in vitro*.** *A*, IB analyses: knockdown of endogenous Ang2 by Ang2.siRNAs (*A*) or a control (*C*) abrogated Ang2-indueced p-Akt^{Ser473} and protein expression of Bcl-2 in MDA-MB-468 and SK-BR-3 cells. Total proteins of Akt and β-actin were used as loading controls. Cell survival (*B*), cell migration (*C*), and apoptosis (*D*) in the cells culture under serum-starvation. Ang2#1 cells were separately transfected siRNA pools for control (*C*) or Ang2 (*A*). 48-h later, the cells were incubated with serum-free/phenol red-free medium (serum-starvation) for 4 days. The numbers of survival cells were analyzed by trypan blue dye exclusion, counted and normalized to the cell number of each group seeded on day 0 (*B*). *C*, transfected MDA-MB-468 or SK-BR-3 cells were seeded into upper wells of in a Boyden chambers with 1×10^5 cell per well. Various cells were allowed to migrate through the 12 μm pore size membranes precoated with gelatin for 12 h at 37 °C. After the membrane was fixed and stained, non-migrating cells were removed. The number of migrating cells was quantified under a microscope as we previously described (10). Impact on cell migration was examined. *D*, cell apoptosis was analyzed using a cell death detection ELISA kit. Data of *B–D* were statistically analyzed using *t* test. *, $p < 0.001$ and error bars: mean $\pm$ S.D. The results of *A–D* are representative from three independent experiments with similar results.

FIGURE 9. **Knockdown of endogenous Ang2 in metastatic MDA-MB-231/#1834 cells inhibits the Akt-Bcl-2 signaling, cell survival, and migration but enhances cell apoptosis *in vitro*.** *A*, IB analyses: knockdown of endogenous Ang2 by Ang2.siRNAs (*A*) or a control (*C*) attenuated p-Akt^{Ser473} and expression of Bcl-2 in clone 1834 cells derived from MDA-MB-231 cells. Total proteins of Akt and β-actin were used as loading controls. Cell survival (*B*), cell migration (*C*), and apoptosis (*D*) in the cell culture under serum-starvation. *B*, Ang2#1 cells were separately transfected siRNA pools for a control or Ang2. 48-h later, various cells were incubated with serum-free/phenol red-free medium (serum starvation) for 4 days. The numbers of survival cells were analyzed by trypan blue dye exclusion, counted, and normalized to the cell number of each group seeded on day 0. *C*, impact on cell migration. Transfected MDA-MB-231/#1834 cells were seeded into upper wells of Boyden chambers with 1×10^5 cells per well. Various cells were allowed to migrate through the 12 μm pore size membranes precoated with gelatin for 12 h at 37 °C. After the membrane was fixed and stained, non-migrating cells were removed. The number of migrating cells was quantified under a microscope as we previously described (10). *D*, cell apoptosis was analyzed using a cell death detection ELISA kit. Data of *B–D* were statistically analyzed using *t* test. *, $p < 0.001$ and error bars: mean $\pm$ S.D. The results of *A–D* are representative from three independent experiments with similar results.

metastasis by promoting the initial tumor cell survival and growth in their new microenvironment through stimulation of the ILK/Akt/Bcl-2 signaling.

Breast cancer metastasis is an inefficient process and each step is equally important for tumor cells to successfully establish metastatic tumors in the targeting organs (2). A number of studies showed that the presence of tumor cells in the blood circulation does not predict whether tumor metastasis will occur because most of the tumor cells that enter the blood stream are rapidly eliminated (2). Our data validated these observations. At the first 4 h after intravenous injection of MCF-7 breast cancer cells into mice, a large number of GFP-expressing tumor cells were retained in the lung, perhaps before, during or after extravasation from the vasculatures. At 12 and 24 h post-injection, near 90% of GFP tumor cells that were initially retained were eliminated in the lung of mice that received Ang2-expressing or GFP-expressing control cells. In control groups, by 48 h, less than 2% of GFP control cells were retained and viable. At 8 days, less than 0.5% GFP control cells were viable (Fig. 2, *A* and *B*). Importantly, these cells failed to survive, proliferate and grow into macrometastatic tumors (Fig. 1, *A* and *B*). In contrast, at 24 h post-injection, Ang2#1 cells displayed a higher retention rate than GFP control cells (Fig.
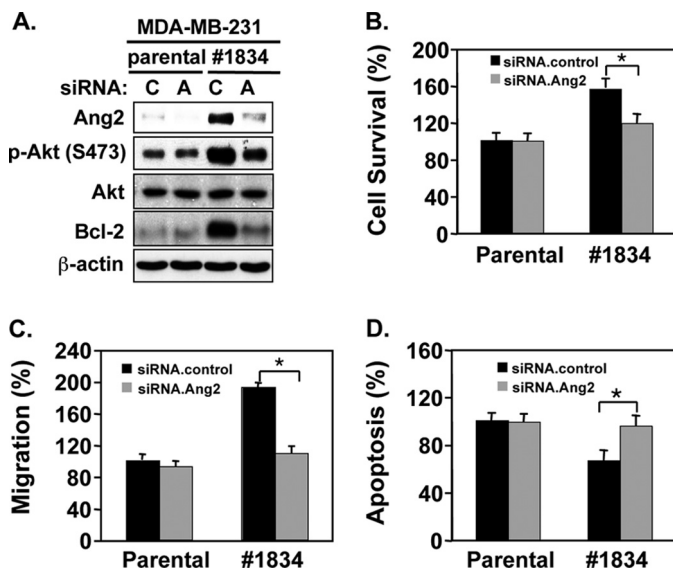
2*B*). Furthermore, from 48 h to 8 days post-injection, Ang2#1 cells not only stayed as small tumor clusters but also started to grow, accompanied a significant decrease in cell apoptosis (Fig. 2, *A–D*). A previous study demonstrated that tumors grow much slower in Ang2-deficient mice compared with that in wild type animals at their early stage growth, suggesting that Ang2 is involved in tumor initiation (29). Our data corroborate with this report. By using an experimental metastasis model, we demonstrate that Ang2 acts on initial steps of breast cancer metastasis through promoting tumor cell retention in the lung and increase cell survival, thereby stimulating breast tumor metastasis to the lung of animals.

Our mechanistic data showed that Ang2 plays a critical role at early stages of breast cancer metastasis in the lung through the ILK/Akt/Bcl-2 pathway. Akt is a key modulator for variety of cellular functions including cell proliferation, growth, protein synthesis, cell metabolism, and survival (25). Although all three Akt isoforms have alterations in clinical breast tumor specimens (30), only Akt1 and Akt2 showed impacts on breast cancer development and metastasis (31). In transgenic mammary gland tumor mouse models, activation of Akt1 accelerates v-erb-b2 erythroblastic leukemia viral oncogene homolog 2 (ErbB2)/Neu-mediated mammary gland tumor development

(32). Moreover, activation of Akt2 markedly enhances mammary gland tumor metastasis to the lung (26). Conversely, ablation of Akt1 inhibits, whereas deficiency in Akt2 accelerates the progression and growth of the ErbB2/neu-mediated mammary carcinoma in mice (33). Additionally, studies using *in vitro* and *in vivo* models further support the notion that Akt1 and Akt2 play distinct roles in modulation of breast cancer progression, growth, invasion, and metastasis (34–37). Our results agree but also differ from these observations. We demonstrate that Akt1 and Akt2, and one of their effectors, Bcl-2 are critical for Ang2-stimulated MCF-7 breast cancer metastasis at the initial onset of metastatic process in the lung of animals. We show that Akt1 and Akt2 but not Akt3 are expressed in MCF-7 cells and Ang2 stimulation induces protein phosphorylation of Akt1 and Akt2 and expression of Bcl-2. Inhibition of Akt1 and Akt2, their direct upstream activator ILK (10) or downstream Bcl-2 (25) abrogates Ang2-stimulated cell survival under stress conditions *in vitro* and in the lung of animals. We also show that knockdown of either Akt1 or Akt2 alone or together have inhibitory impacts on Ang2-stimulated cell survival under stress conditions *in vitro*. Although these data does not differentiate whether Akt1 and Akt2 play distinct roles in the early onset of breast cancer metastasis in the lung, our observations warrant further investigation to study how Akt1 and Akt2 affect Ang2- or other stimuli-promoted pulmonary metastasis of breast cancers. Finally, we detected high levels of endogenous Ang2 proteins in two breast cancer cell lines, MDA-MB-468 and SK-BR-3 (17) and MDA-MB-231/#1844 cells that are highly metastatic to the lung (18). Knockdown of the endogenous Ang2 in these cells inhibited stimulated Akt/Bcl-2 signaling, cell survival, migration and increased cell apoptosis, further demonstrating the role of Ang2 in promoting breast cancer cell survival, migration and suppressing cell apoptosis through the Akt-Bcl-2 signaling.

In summary, this study investigates the mechanisms of Ang2 stimulation of breast cancer lung metastasis at early stages. By using an experimental tumor metastasis model, we reveal that that Ang2 enhances breast cancer cell survival and suppresses cell apoptosis under growth stress conditions through the ILK/Akt/Bcl-2-mediated signal pathway, thereby promoting breast cancer metastasis to the lung and several other organs of animals. We show that ILK, Akt1, and Akt2 as well as Bcl-2 are critical for the enhanced breast cancer cell survival and tumor metastasis in the lung. Because high levels of Ang2 expression is closely linked with increased potential of angiogenesis, tumor growth, and metastasis of breast cancers, our data suggest Ang2 as a promising therapeutic target for treating patients with metastatic breast cancers.

REFERENCES

1. Jemal, A., Siegel, R., Xu, J., and Ward, E. (2010) *CA: A Cancer Journal for Clinicians* **60,** 277–300
2. Chambers, A. F., Groom, A. C., and MacDonald, I. C. (2002) *Nat. Rev. Cancer* **2,** 563–572
3. Weigelt, B., Peterse, J. L., and van 't Veer, L. J. (2005) *Nat. Rev. Cancer* **5,** 591–602
4. Nguyen, D. X., Boss, P. D., and Massagué, J. (2009) *Nat. Rev. Cancer* **9,** 274–284
5. Tallmadge, J. E., and Fidler, I. J. (2010) *Cancer Res.* **70,** 5649–5669
6. Huang, H., Bhat, A., Woodnutt, G., and Lappe, R. (2010) *Nat. Rev. Cancer* **10,** 575–585
7. Thomas, M., and Augustin, H. G. (2009) *Angiogenesis* **12,** 125–137
8. Helfrich, I., Edler, L., Sucker, A., Thomas, M., Christian, S., Schadendorf, D., and Augustin, H. G. (2009) *Clin. Cancer Res.* **15,** 1384–1392
9. Hu, B., and Cheng, S. Y. (2009) *Curr. Oncol. Rep.* **11,** 111–116
10. Imanishi, Y., Hu, B., Jarzynka, M. J., Guo, P., Elishaev, E., Bar-Joseph, I., and Cheng, S. Y. (2007) *Cancer Res.* **67,** 4254–4263
11. Oliner, J., Min, H., Leal, J., Yu, D., Rao, S., You, E., Tang, X., Kim, H., Meyer, S., Han, S. J., Hawkins, N., Rosenfeld, R., Davy, E., Graham, K., Jacobsen, F., Stevenson, S., Ho, J., Chen, Q., Hartmann, T., Michaels, M., Kelley, M., Li, L., Sitney, K., Martin, F., Sun, J. R., Zhang, N., Lu, J., Estrada, J., Kumar, R., Coxon, A., Kaufman, S., Pretorius, J., Scully, S., Cattley, R., Payton, M., Coats, S., Nguyen, L., Desilva, B., Ndifor, A., Hayward, I., Radinsky, R., Boone, T., and Kendall, R. (2004) *Cancer Cell* **6,** 507–516
12. Falcón, B. L., Hashizume, H., Koumoutsakos, P., Chou, J., Bready, J. V., Coxon, A., Oliner, J. D., and McDonald, D. M. (2009) *Am. J. Pathol.* **175,** 2159–2170
13. Brown, J. L., Cao, Z. A., Pinzon-Ortiz, M., Kendrew, J., Reimer, C., Wen, S., Zhou, J. Q., Tabrizi, M., Emery, S., McDermott, B., Pablo, L., McCoon, P., Bedian, V., and Blakey, D. C. (2010) *Mol. Cancer Therap.* **9,** 145–156
14. Chae, S. S., Kamoun, W. S., Farrar, C. T., Kirkpatrick, N. D., Niemeyer, E., de Graaf, A. M., Sorensen, A. G., Munn, L. L., Jain, R. K., and Fukumura, D. (2010) *Clin. Cancer Res.* **16,** 3618–3627
15. Coxon, A., Bready, J., Min, H., Kaufman, S., Leal, J., Yu, D., Lee, T. A., Sun, J. R., Estrada, J., Bolon, B., McCabe, J., Wang, L., Rex, K., Caenepeel, S., Hughes, P., Cordover, D., Kim, H., Han, S. J., Michaels, M. L., Hsu, E., Shimamoto, G., Cattley, R., Hurh, E., Nguyen, L., Wang, S. X., Ndifor, A., Hayward, I. J., Falcón, B. L., McDonald, D. M., Li, L., Boone, T., Kendall, R., Radinsky, R., and Oliner, J. D. (2010) *Mol. Cancer Therap.* **9,** 2641–2651
16. Hashizume, H., Falcón, B. L., Kuroda, T., Baluk, P., Coxon, A., Yu, D., Bready, J. V., Oliner, J. D., and McDonald, D. M. (2010) *Cancer Res.* **70,** 2213–2223
17. Niu, G., and Carter, W. B. (2007) *Cancer Res.* **67,** 1487–1493
18. Minn, A. J., Gupta, G. P., Siegel, P. M., Bos, P. D., Shu, W., Giri, D. D., Viale, A., Olshen, A. B., Gerald, W. L., and Massagué, J. (2005) *Nature* **436,** 518–524
19. Hu, B., Guo, P., Fang, Q., Tao, H. Q., Wang, D., Nagane, M., Huang, H. J., Gunji, Y., Nishikawa, R., Alitalo, K., Cavenee, W. K., and Cheng, S. Y. (2003) *Proc. Natl. Acad. Sci. U.S.A.* **100,** 8904–8909
20. Bianchi, L., Tacchini, L., and Cairo, G. (1999) *Nucleic Acids Res.* **27,** 4223–4227
21. Fukuda, T., Chen, K., Shi, X., and Wu, C. (2003) *J. Biol. Chem.* **278,** 51324–51333
22. Stahl, J. M., Sharma, A., Cheung, M., Zimmerman, M., Cheng, J. Q., Bosenberg, M. W., Kester, M., Sandirasegarane, L., and Robertson, G. P. (2004) *Cancer Res.* **64,** 7002–7010
23. Cascio, S., Bartella, V., Auriemma, A., Johannes, G. J., Russo, A., Giordano, A., and Surmacz, E. (2008) *Oncogene* **27,** 540–547
24. Hannigan, G., Troussard, A. A., and Dedhar, S. (2005) *Nat. Rev. Cancer* **5,** 51–63
25. Manning, B. D., and Cantley, L. C. (2007) *Cell* **129,** 1261–1274
26. Dillon, R. L., Marcotte, R., Hennessy, B. T., Woodgett, J. R., Mills, G. B., and Muller, W. J. (2009) *Cancer Res.* **69,** 5057–5064
27. Arisan, E. D., Kutuk, O., Tezil, T., Bodur, C., Telci, D., and Basaga, H. (2010) *Breast Cancer Res. Treat* **119,** 271–281
28. Kang, Y., Siegel, P. M., Shu, W., Drobnjak, M., Kakonen, S. M., Cordón-Cardo, C., Guise, T. A., and Massagué, J. (2003) *Cancer Cell* **3,** 537–549
29. Nasarre, P., Thomas, M., Kruse, K., Helfrich, I., Wolter, V., Deppermann, C., Schadendorf, D., Thurston, G., Fiedler, U., and Augustin, H. G. (2009) *Cancer Res.* **69,** 1324–1333
30. Kirkegaard, T., Witton, C. J., Edwards, J., Nielsen, K. V., Jensen, L. B.,

Campbell, F. M., Cooke, T. G., and Bartlett, J. M. (2010) *Histopathology* **56,** 203–211

31. Dillon, R. L., and Muller, W. J. (2010) *Cancer Res.* **70,** 4260–4264
32. Hutchinson, J. N., Jin, J., Cardiff, R. D., Woodgett, J. R., and Muller, W. J. (2004) *Cancer Res.* **64,** 3171–3178
33. Maroulakou, I. G., Oemler, W., Naber, S. P., and Tsichlis, P. N. (2007) *Cancer Res.* **67,** 167–177
34. Arboleda, M. J., Lyons, J. F., Kabbinavar, F. F., Bray, M. R., Snow, B. E., Ayala, R., Danino, M., Karlan, B. Y., and Slamon, D. J. (2003) *Cancer Res.* **63,** 196–206
35. Sun, M., Paciga, J. E., Feldman, R. I., Yuan, Z., Coppola, D., Lu, Y. Y., Shelley, S. A., Nicosia, S. V., and Cheng, J. Q. (2001) *Cancer Res.* **61,** 5985–5991
36. Wang, J., Wan, W., Sun, R., Liu, Y., Sun, X., Ma, D., and Zhang, N. (2008) *Cellular signalling* **20,** 1025–1034
37. Iliopoulos, D., Polytarchou, C., Hatziapostolou, M., Kottakis, F., Maroulakou, I. G., Struhl, K., and Tsichlis, P. N. (2009) *Science Signaling* **2,** ra62